ELSEVIER

Chemical Engineering Journal 131 (2007) 217–224

Chemical Engineering Journal

www.elsevier.com/locate/cej

Influence of the processing variables on the performance of MAGCLA™ Part I: Blank simulation

Paulo A. Augusto [a,b,*], Teresa Castelo-Grande [a], Domingos Barbosa [a], A.M. Estévez [b]

[a] *Departamento de Engenharia Química, Faculdade de Engenharia da Universidade do Porto, Rua Dr. Roberto Frias, 4200-465 Porto, Portugal*
[b] *Departamento de Ingeniería Química y Textil, Facultad de Ciencias Químicas, Universidad de Salamanca, Plaza de los Caídos 1-5, 37008 Salamanca, Spain*

Received 19 June 2006; received in revised form 3 November 2006; accepted 19 November 2006

Abstract

Current magnetic separators are only able to split the feed into three different streams. In this work we simulate the behavior of different particles in a new magnetic-classifier, named MAGCLA™, which is capable to separate and classify particles according to their magnetic susceptibilities. In this first part of the work the results for a blank simulation are reported. This study is the mandatory basis of comparison for the assessment of the influence of the process variables in the outcome results. These comparative studies will be reported in future works.

Keywords: Magnetic classification; Magnetic separation; Separations; Materials processing; Particle processing; Simulation

1. Introduction

Although traditionally considered a minerals processing technique, magnetic separation is very often applied to several other areas of science and technology (e.g., chemical engineering [1], environmental engineering [2], health sciences [3], etc.). Even though its application in minerals processing industries has already reached high levels of efficiency, these industrial separators are unable to reach a *differential classification* of the several magnetic species present in the feed [4,5]. In fact, they are only able to split the feed into three different product streams [6]: the *Mags*, containing the particles presenting the highest magnetic susceptibility (strong paramagnetic, ferromagnetic), the *Tails*, which contain the particles presenting the lowest magnetic susceptibility (weak paramagnetic, diamagnetic), and the *Middlings*, containing the remaining particles (particles presenting intermediate susceptibility—paramagnetic particles or agglomerated mixtures of particles). We have developed a new magnetic separator and classifier, named MAGCLA™ [7,8], which is able to achieve the differential magnetic classification of magnetic particles (i.e., separation of the particles by classes of magnetic susceptibility [4,5]) and a large-scale prototype of the device is being currently constructed for testing [9]. This device may operate with a rotating or static conical-trunk and with dry or aqueous feeds (i.e., in dry or wet mode). Fig. 1 describes the fundamental components of the device designed for the processing of minerals, although its applications are not restricted to this area [9,10]. The supporting theory of the new device – concerning the equations of movement, modeling and limiting conditions of operation for all the particles present in the device – is described in previous works [11–14], regarding its application for minerals processing industries for dry mode and rotating trunk operation.

In this work the behavior for a specific system will be simulated in order to establish a blank test that will be used as basis for comparison in subsequent papers. To reach this goal, the supporting theory of MAGCLA™ [11–14] will be used to simulate the real paths followed by the particles in this new device. In three subsequent papers we will describe the influence of the processing variables on the performance of MAGCLA™, namely: angle of the trunk, α, speed of rotation, ω, friction coefficient, μ, radius of the particles, r_{part}, current intensity, I, and real feeding radius, $r_{\text{R}} - T_{\text{CG}} r_{\text{i}}$.

2. Working principles of the new device

Detailed descriptions of the new apparatus working principles can be found in previous works [7,8,11,15]. In this section,

* Corresponding author. Tel.: +351 93 824 43 14.
E-mail address: pauloaugusto@ieee.org (P.A. Augusto).

1385-8947/$ – see front matter © 2006 Elsevier B.V. All rights reserved.
doi:10.1016/j.cej.2006.11.013

Nomenclature

a	acceleration of the particle (m/s^2)
a_r	acceleration in the r direction (m/s^2)
a_{rt}	tangential acceleration of the particle (m/s^2)
a_t	total acceleration (m/s^2)
a_z	acceleration in the z direction (m/s^2)
a_θ	acceleration on the θ direction (m/s^2)
A	cross-sectional area of the particle (m^2)
C_d	drag coefficient
F_{at}	friction force (N)
F_c	centrifugal force (N)
F_D	drag force (N)
F_{mag}	magnetic force (N)
g	gravity acceleration (m/s^2)
h_f	height of the conical part of the body of the separator–classifier (m)
h_i	initial height of the fed particles (m)
I	overall current intensity flowing in the superconducting cable (A)
m	mass of the particle (kg)
nvolt	number of turns given by the particles in the surface of the device
N	reaction of the surface (N)
P	weight (N)
r	radial distance between the particle and the geometrical center (m)
r_a	radius of the cylindrical part of the body of the separator–classifier (m)
r_c	external radius of the central collector (m)
r_f	internal radius of the conical part of the body of the separator–classifier (m)
r_i	initial radius of the fed particles (m)
r_{lv}	radius at which magnetic particles depart towards the center (m)
r_{part}	radius of the particle (m)
r_R	fictitious radius to account for the deviations to ideality (m)
r_{tic}	radius of the superconducting magnet plus cryostat system (m)
t	time (s)
t_c	time of arrival of the magnetic particles at the central collector (s)
T_{CG1} and T_{CG2}	theoretical adimensional parameters that measure the disparities between theory and practice
t_f	time of arrival of the magnetic particles at the largest radius of the trunk (r_f) (s)
t_{lv}	time at which magnetic particles depart towards the central collector (s)
v_p	velocity of the particle in the direction of the movement (m/s)
v_{pt}	velocity of the particle in the tangential direction of the circular movement (m/s)
v_r	velocity in the r direction (m/s)
v_{rc}	velocity of the magnetic particles in the r direction at the moment of arrival at the central collector (m/s)
v_{rlv}	velocity of particle in the r direction at the moment when the magnetic particles depart towards the central collector (m/s)
v_{rt}	total velocity of the particle in the r direction (m/s)
v_t	total velocity of the particle (m/s)
v_{tc}	total velocity of the particle at the moment of arrival at the central collector (m/s)
v_{tlv}	velocity of particle in the *tangential* direction at the moment when the magnetic particles depart towards the central collector (m/s)
v_{Tlv}	total velocity of particle at the moment when the magnetic particles depart towards the central collector (m/s)
v_z	velocity in the z direction (m/s)
v_{zc}	velocity of particle in the z direction at the moment when the magnetic particles arrive at the central collector (m/s)
v_{zlv}	velocity of particle in the z direction at the moment when the magnetic particles depart towards the central collector (m/s)
v_θ	velocity of the particle in the the θ direction (m/s)
$v_{\theta lv}$	velocity of the particle in the the θ direction at the moment when the magnetic particles depart towards the central collector (m/s)
Vol_p	volume of the particles (m^3)
z	height displacement (m)
z_c	height of arrival of the magnetic particles in the central collector (m)
z_{lv}	height at which magnetic particles depart towards the central collector (m)

Greek letters

α	angle between the body of the separator–classifier and the horizontal (°)
β	angle between the total velocity and the radial velocity (third part of the movement) (°)
β_c	angle between the total velocity and the radial velocity, at the moment of arrival of the magnetic particles in the central collector (°)
χ	magnetic susceptibility of the particle (m^3/kg)
χ_{base}	lowest value of the magnetic susceptibility that the magnetic particles must possess in order to depart towards the central collector (thus being classified) before reaching radius r_a where they will fall into the base collector (m^3/kg)
$\chi_{maxclas}$	highest value of the magnetic susceptibility that the magnetic particles must possess in order to be classified at the central collector, as all the particles presenting a magnetic susceptibility value higher than $\chi_{maxclas}$ will be collected at the same level in the central collector, therefore not being classified differentially (m^3/kg)

χ_{min}	lowest value of the magnetic susceptibility that the magnetic particles must possess in order to be separated from the non-magnetic ones at the feeding radius (m^3/kg)
φ	angle between the total velocity and the rotational axis (°)
φ_{lv}	angle between the total velocity and the rotational axis, at the moment when the particles depart towards the central collector (°)
μ	friction coefficient for the surface of the separator–classifier on the tangential direction
μ_{tang}	friction coefficient in the *tangential* direction
μ_θ	friction coefficient in the θ direction
μ_0	vacuum permeability (T m/A)
$\theta(t)$	rotational displacement (°)
$\theta_{lv}(t)$	rotational displacement, at the moment when the particles depart towards the central collector (°)
ρ_f	density of the fluid (kg/m^3)
ρ_p	density of the particle (kg/m^3)
ω	angular velocity of the body of the MAGCLA™ (rad/s)

only a very brief description will be presented. The feeding system delivers the initial mixture of particles present in the feed stream to the conical-trunk surface; at the delivery point they suffer the simultaneous action of the drag force

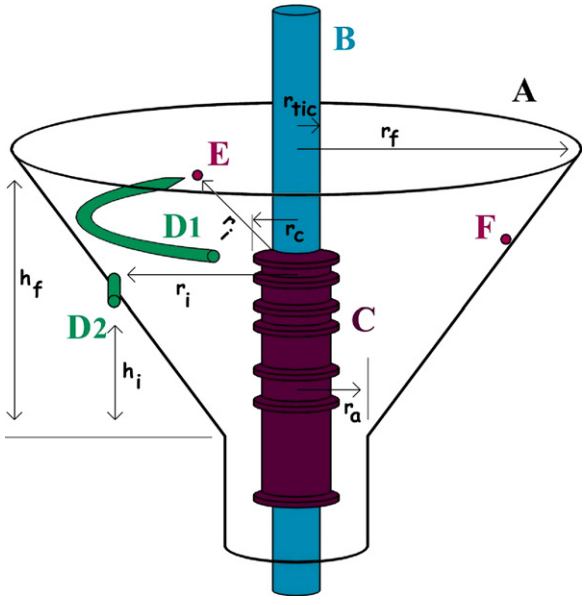

Fig. 1. Schematic representation of the new magnetic separator and classifier: A, body (rotating or non-rotating); B, superconducting magnet; C, central collector; D1 and D2, feeding systems; E, particle fed at the initial radius r_i; F, particle being separated and classified; h_f, height of the conical part of the body of the separator–classifier; h_i, initial height of the fed particles; r_a, radius of the cylindrical part of the body of the separator–classifier; r_c, external radius of the central collector; r_f, internal radius of the conical part of the body of the separator–classifier; r_i, initial radius of the fed particles; r_{tic}, radius of the superconducting magnet plus cryostat system.

($F_D = mC_d(A/Vol_p)(\rho_f/\rho_p)(v_p^2/2)$ [12]), weight ($P = Vol_p(\rho_p - \rho_f)g = mg$ [11]), friction force ($F_{at} = \mu N$), magnetic force (caused by the action of the magnetic field generated by the central superconducting magnet) ($|F_{mag}| = m\chi(\mu_0 I^2/4\pi^2 r^3)$ [12]), and centrifugal force (caused by the rotation of the trunk) ($F_c = Vol_p((\rho_p - \rho_f)/r)v_{pt}^2 = m\omega^2 r$ [11]). These two latter forces act on the same axis but in opposite directions; therefore, if the speed of rotation is high enough, the particles with lower magnetic susceptibilities or diamagnetic properties raise upon the surface of the device (their centrifugal force is higher than the weight component and mainly higher than the magnetic force acting in the opposite direction – in the diamagnetic case this force may act on a different direction – and as derived from the equation defining the centrifugal force, they will feel a increasingly stronger centrifugal force while rising upon the surface), while the magnetic particles presenting higher magnetic susceptibility (strong ferromagnetic) depart towards the center of the device (as their magnetic force magnitude is much higher than the opposing centrifugal and drag forces), and the magnetic particles presenting magnetic susceptibility within certain limits (which are controlled by the operating variables) descend upon the surface of the device (their magnetic force is stronger than the opposing centrifugal and drag forces, but not so strong as to make the particles fly immediately towards the central collector, as in the case of the ferromagnetic particles). During their fall, these latter particles will suffer the influence of an increasingly stronger magnetic field, which will increase the strength of the magnetic forces, while the other forces will remain comparatively constant or with a very low increase/decrease. As this magnetic force is dependent upon the magnetic susceptibility of the particles, at the same radius, the magnetic particles with higher magnetic susceptibilities will feel a higher magnetic force than the other ones, and therefore the magnetic particles will depart towards the center at different heights according to their magnetic susceptibility (see [8,12]). Different collecting systems are used to collect the particles: a central collector gathers the particles according to their magnetic susceptibilities (classification), a top collector assembles the diamagnetic particles and the paramagnetic particles presenting very low magnetic susceptibilities, and a bottom collector retains the particles presenting low magnetic susceptibilities (that are separated at the feeding point, but that do not present high enough magnetic susceptibility in order to be classified during their descent).

The discrepancies between the real and the theoretical behavior of the particles have been taken in account by two coefficients – T_{CG1} and T_{CG2} – which are described in previous works [11,12].

3. Blank simulation for the determination of the influence of the processing variables

3.1. Introduction

In order to determine the influence of each processing parameter in the magnetic classification and separation process outcomes, the parameter under study was varied while keeping constant all the other parameters. The ideal procedure was to

Table 1
Values of the constant parameters considered in the simulations

Universal parameters	
g (m/s^2)	9.80665
μ_0 (Tm/A)	$4\pi \times 10^{-7}$
Geometrical parameters	
r_c (cm)	12
r_a (cm)	15
r_f (cm)	45
Parameters of the particles	
C_d	0.27
Parameters of the fluid	
ρ_f (kg/m^3)	1.24

g is the medium value of the gravity acceleration, μ_0 the vacuum permeability, r_a the radius of the cylindrical section of the body of the separator–classifier, r_c the external radius of the central collector (for the magnetic particles), r_f the maximum internal radius of the conical-section of the body of the separator–classifier, C_d the drag coefficient of the particles, and ρ_f is the specific weight of the fluid.

be able to vary all the parameters simultaneously, but this is a very complicated situation, if not impossible, to analyze. In fact, the optimization-goal varies from case to case, depending exclusively upon the choice of the operator. Thus, we consider that the methodology followed not only allows the analysis of the influence of each variable, but also to obtain the spectrum of values advisable for an optimum performance of the separator–classifier.

The six parameters considered in this study are: the angle between the body of the separator–classifier and the horizontal line, α, the speed of rotation of the body of the separator–classifier, ω, the friction coefficient acting on the upwards/downwards direction, μ, the radius of the particles, r_{part}, the electrical current intensity supplied to the superconducting magnet, I, and the real feeding radius, r_R (=$T_{CG}r_i$). The remaining parameters were considered constant, and their values picked within their standard or required spectrum of values (see Table 1).

The optimization-goal (although it varies from case to case) was generically considered (only for comparison purposes) as the separation and classification of the largest possible spectrum of magnetic susceptibilities. It was also considered as optimization-goal, in what concerns magnetic particles, the separation and classification of wolframite particles present in the feed with 100% purity.

The friction coefficient in the rotational direction (μ_θ) was always considered above the limiting value given by the theory [13,14]. In order to introduce a safety factor in our calculations, and regarding this late approach, we have considered for the minimum radius, until which the "gluing" condition must be maintained, an extra 5% relatively to the value of the lift-off radius (r_{lv}).

For each variable study and for the blank simulation we only present in this papers the final results obtained for the values considered for the processing variable under analysis and for the values considered in the case of the blank simulation; the detailed partial results may be found in Ref. [5].

3.2. "Blank" simulation

For a better comparison of the results of the simulations we have always considered a typical separation process, the blank simulation, which will be used in future works. For this blank simulation we have considered that our feed was only constituted by generical non-magnetic particles and by wolframite particles 100% pure. As the first optimization-goal of this blank simulation we have considered the separation between the non-magnetic particles and the particles of wolframite 100% pure, and as the second optimization-goal we have considered that after the initial separation the wolframite particles would descend on the surface of the trunk of the MAGCLA^{TM} for a while, and at a certain radius (r_{lv}) would be classified and thus "lift-off" towards the central collector, where they would be collected at a certain height.

The main characteristics of the particles (magnetic and non-magnetic) considered were typical ones (and are presented in Tables 1 and 2) and the values considered for the processing variables in this blank simulation are summarized in Table 2. The latter were chosen in order to achieve the two optimization-goals, and at the same time allowing the future variation of the values of these processing variables (in the simulations of the determination of the influence of the processing variables). The limiting conditions considered and the minimum values required for the rotational friction factor are also presented.

The results were divided into two main categories: non-magnetic and magnetic particles. Bearing in mind the magnetic particles, the results obtained for the two main stages of the movement were also presented: movement of the parti-

Table 2
Values used in the blank simulation for the main processing variables, and limiting conditions followed

Material: Wolframite										
α	ω (rad/s)	μ_{tang}	μ_θ	r_{part} (μm)	I (A)[a]	r_i (cm)	T_{CG1}	T_{CG2}	ρ_p (kg/m^3)	χ (m^3/kg)[a]
30°	6	0.2	≥19	100	3×10^6	30	0.95	1.05	7510	1.2×10^{-6}
Limiting conditions followed [12,13]: [(CNM1.2), (CNM1.4), (CNM2), (CNM3)], [(A15), (A21)][b]										

α is the angle between the body of the separator–classifier and the horizontal, ω the speed of rotation of the body of the separator–classifier, μ_{tang} the friction coefficient in the upwards/downwards direction, μ_θ the friction coefficient in the rotational direction, r_{part} the radius of the particles, I the electrical current intensity supplied to the superconducting magnet, r_i the initial feeding radius, T_{CG1} and T_{CG2} the transition coefficients between ideality and practical reality, ρ_p the density of the particles and χ their magnetic susceptibility.

[a] Only concerning magnetic particles.

[b] As referred in Refs. [12,13], some limiting conditions contain others, and therefore the most limiting conditions are presented and followed.

cles upon the surface of the body of the separator–classifier and movement of the particles in flight towards the central collector.

The values in percentage refer to the degree of purity of the wolframite particles – typical case – which are separated considering the values of the processing variables in question. This percentage was computed considering that the magnetic susceptibility of pure wolframite particles (100% pure) is 12×10^{-7} m^3/kg.

3.2.1. Non-magnetic particles

The trajectories followed by the non-magnetic particles, obtained by simulation considering the parameters given in Tables 1 and 2, are shown in Fig. 2. The paths are presented for different elapsed time periods. Fig. 2F presents the complete path followed by the non-magnetic particles from the time they are fed until they reach the radius r_f ($t_f \approx 0.45$ s). The time t_f required for a non-magnetic particle to reach the top of the trunk of the separator–classifier (starting from the

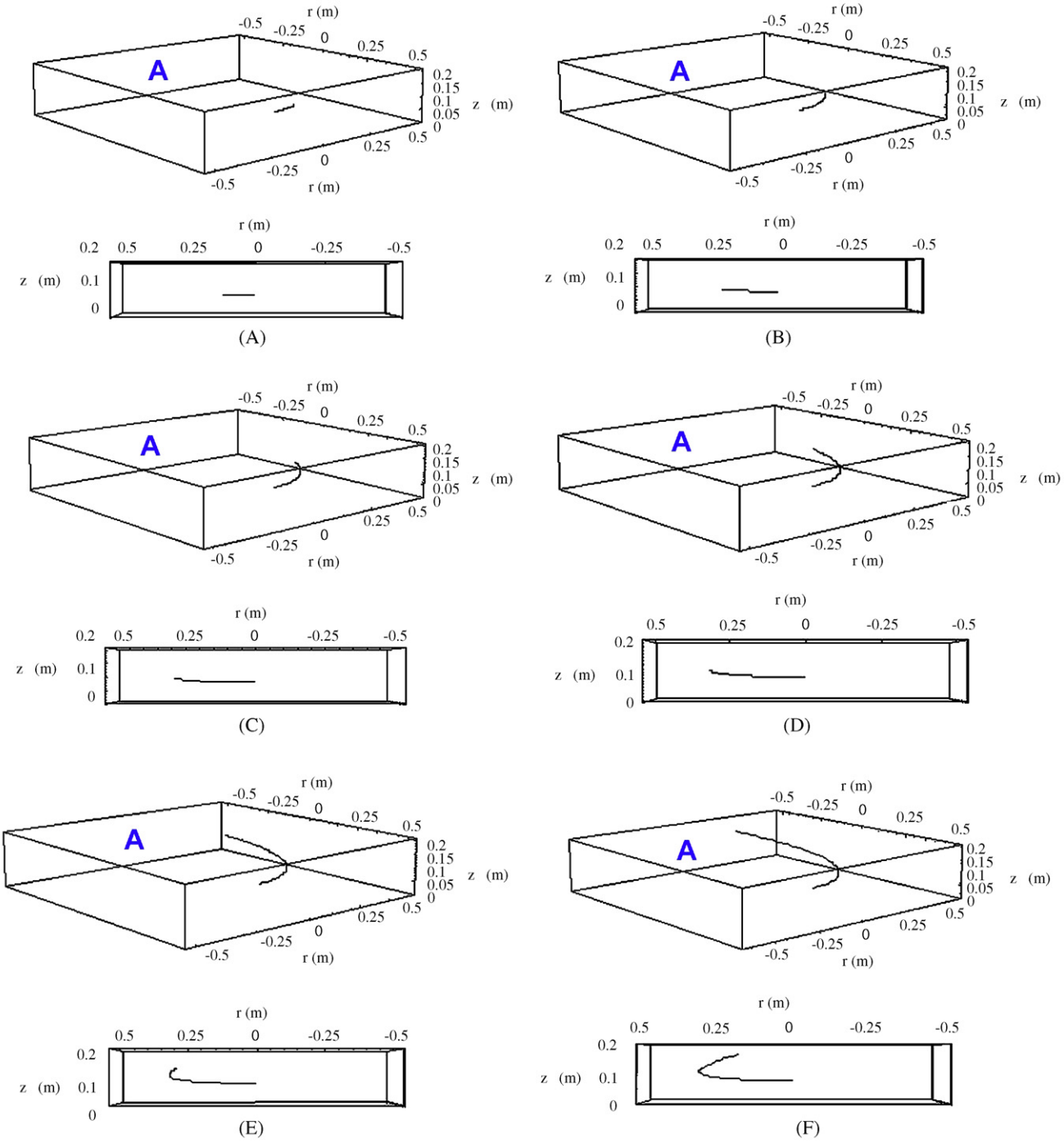

Fig. 2. Trajectories followed by the non-magnetic particles (tri-dimensional and side views), for: (A) $\Delta t = 0.075$ s; (B) $\Delta t = 0.151$ s; (C) $\Delta t = 0.226$ s; (D) $\Delta t = 0.302$ s; (E) $\Delta t = 0.377$ s; (F) $\Delta t = 0.452$ s. The side view graphics are seen from the surface A of the tri-dimensional ones.

Table 3
Simulated results obtained for the blank simulation concerning the non-magnetic particles

r (m); v_z (m/s)	z (m); v_θ (m/s)	θ; v_T (m/s)	nvolt; φ	v_{rt} (m/s); a_{rt} (m/s^2)	v_r (m/s)
$t = t_f/6 = 0.075$ s					
0.288; 0.048	0.080; 1.729	25.9°; 1.732	0; 3.211°	0.097; 1.344	0.084
$t = t_f/3 = 0.151$ s					
0.298; 0.104	0.085; 1.788	51.9°; 1.800	0; 6.615°	0.207; 1.615	0.180
$t = t_f/2 = 0.226$ s					
0.316; 0.173	0.096; 1.895	77.8°; 1.926	0; 10.351°	0.346; 2.108	0.300
$t = 2 \times t_f/3 = 0.302$ s					
0.344; 0.266	0.112; 2.065	104°; 2.133	0; 14.458°	0.532; 2.890	0.461
$t = 5 \times t_f/6 = 0.377$ s					
0.387; 0.396	0.137; 2.322	130°; 2.453	0; 18.834°	0.792; 4.069	0.686
$t = t_f = 0.452$ s					
0.450; 0.580	0.173; 2.700	156°; 2.939	0; 23.254°	1.160; 5.808	1.005

Output variables as defined in Ref. [11].

feeding radius and ending at the larger radius of the trunk of the separator–classifier, $r_f = 0.45$ m, see Fig. 1) was computed solving Eq. 3.18 in Ref. [11] bearing in mind the boundary condition $t = t_f \Rightarrow r = r_f$. It is interesting to notice the ascending path of the particles on the trunk, namely that they only describe half of a turn before exiting the trunk, and that the path is as expected.

Table 3 summarizes the values obtained for all the relevant variables, for the final time t_f and five time values in between. Notice the low value of the exiting time of the non-magnetic particles, and the moderately high velocities of ascension and exiting, and also the continuously increasing deflection angle, and acceleration values. These results show that part of the first optimization-goal was achieved, and they also indicate that the values chosen for the parameters and variables are appropriate for a blank simulation, has they induce that there is enough margin to vary the processing variables in future works (in order to determine the influence of the processing variables in MAGCLA^{TM} performance), and that the blank simulation represents a good comparison case.

3.2.2. Magnetic particles

In the case of magnetic particles is important to define the following variables (see [16]): χ_{min}, the lowest value of the magnetic susceptibility that the magnetic particles must possess in order to be separated from the non-magnetic ones at the feeding radius (and which corresponds to a certain degree of purity); χ_{base}, the lowest value of the magnetic susceptibility (which corresponds to a certain degree of purity) that the magnetic particles must possess in order to depart towards the central collector (allowing their classification) before reaching radius r_a, at which they will fall into the base collector; $\chi_{maxclas}$, the highest value

Table 4
Blank simulation results of the magnetic particles movement

χ_{minrR} (m^3/kg)	χ_{base} (m^3/kg)	r_{lv} (m)	z_{lv} (m)	θ_{lv}	nvolt	t_{lv} (s)
Part 1						
8.753×10^{-7} (72.94%)	2.637×10^{-7} (21.98%)	0.238	0.051	69°	0	0.201

$\chi_{maxclas}$ (m^3/kg)	v_{tlv} (m/s)	v_{rlv} (m/s)	v_{zlv} (m/s)	$v_{\theta lv}$ (m/s)	v_{Tlv} (m/s)	φ_{lv}
Part 1						
2.619E−6	1.324	1.147	0.662	1.427	1.947	43°

r_c (m)	z_c (m)	t_c (s)	v_{rc} (m/s)	v_{zc} (m/s)	v_{Tc} (m/s)	β_c
Part 2						
0.12	0.002	0.254	4.339	1.175	4.495	15.154°

r (m)	z (m)	t (s)	r (m)	z (m)	t (s)
Part 2—intermediate results					
0.220	0.041	0.214	0.150	0.011	0.246
0.200	0.031	0.226	0.140	0.008	0.249
0.180	0.022	0.235	0.130	0.005	0.251
0.160	0.015	0.242			

Output variables as defined in Ref. [12]. Movement of the particles: *part* 1, while on the surface of the trunk of the separator–classifier; *part* 2, while in flight towards the central collector.

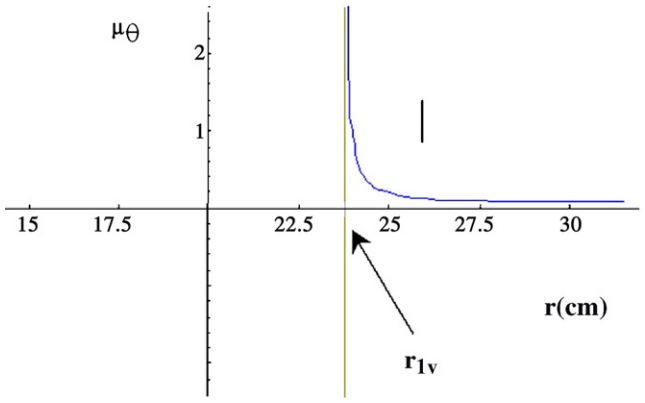

Fig. 3. Value of the required friction coefficient in the θ direction vs. r. The interception of the line with the r axis corresponds to r_{lv} (=23.8 cm).

of the magnetic susceptibility that the magnetic particles must possess in order to be classified at the central collector, as all the particles having a magnetic susceptibility value higher than $\chi_{maxclas}$ will be collected at the same level in the central collector, and therefore will not be classified differentially.

Table 4 presents the results obtained for the simulations carried out for the magnetic particles, with the values of the parameters and variables presented in Tables 1 and 2. In Fig. 3 a graphical method for the determination of the r_{lv} (the radius at which the magnetic particles depart towards the central collector, dividing the movement of the magnetic particles into two main parts [11–14]) value is given (this is based on the depiction of the friction value required to maintain the particles glued to the surface of the trunk [14]). The bi-dimensional simulated trajectories for magnetic particles in question are shown in Fig. 4. In Fig. 5 is presented a graphical depiction of the distribution of the magnetic force density in the separator–classifier created by the value of electrical current density considered in this case (3×10^6 A).

Regarding the results present in Table 4 and Fig. 4, notice:

(a) That with the values chosen for the processing variables, the lowest value of the magnetic susceptibility which the magnetic particles must possess in order to be separated from the non-magnetic ones at the feeding radius, corresponds to 8.753×10^{-7} m^3/kg (which correspond to a degree of

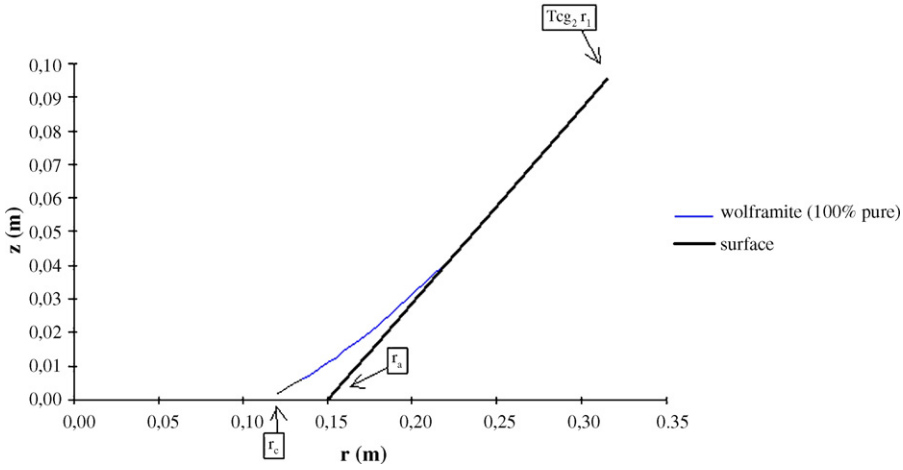

Fig. 4. Bi-dimensional trajectories followed by the Wolframite magnetic particles (100% pure). The displacement in the θ direction was considered negligible (see [12]). r_a is the radius of the cylindrical part of the body of the separator–classifier trunk and r_c is the external radius of the magnetic particles central collector.

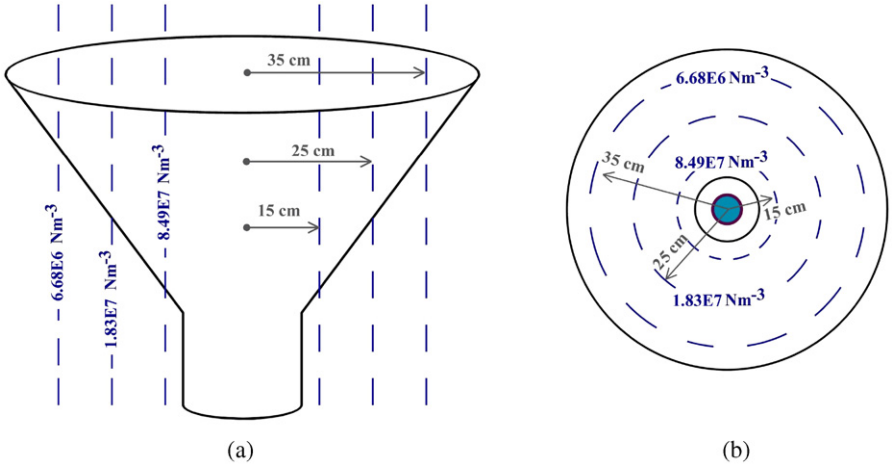

Fig. 5. Volume distribution of the magnetic force density in the separator–classifier for an electrical current density of 3×10^6 A: (a) tri-dimensional view; (b) top view.

purity of 72.94%), which is higher than χ_{base}, the lowest value of the magnetic susceptibility that the magnetic particles must possess in order to depart towards the central collector (allowing their classification) before reaching radius r_a, thus implying that if any other particles of different purity were present in the feed, all the ones with a purity higher than 72.94% would be separated and classified; the highest value of the magnetic susceptibility that the magnetic particles must possess in order to be classified at the central collector corresponds to 2.619×10^{-6} m^3/kg, much higher than the magnetic susceptibility of pure wolframite, therefore the latter will suffer classification.

(b) The low value of the lift-off time of the magnetic particles (during the trajectory supported upon the trunk), and the moderately high velocities and deflection angle they present at the radius of "lift-off" (r_{lv}).

(c) The very low value of the flight time of the magnetic particles (from the moment they lift-off from the trunk until they reach the central collector), and the moderately high velocities they present in the arrival at the central collector.

(d) The detaching path that the magnetic particles follow in the second part of their movement, and the height at which they are collected.

These results show that the second and part of the first optimization-goals were achieved, and as before (in the non-magnetic case) they indicate that the values chosen for the parameters and variables are appropriate for a blank simulation, has they induce that there is enough margin to vary the processing variables in future works (in order to determine the influence of the processing variables in MAGCLA^{TM} performance), and that the blank simulation represents a good comparison case.

4. Discussion of the results and conclusions

In this part of the work we report the results obtained for the blank simulation, which will be the basis of comparison in future parts of this work, when we will analyze the influence of the main processing variables on the performance of the new magnetic separator and classifier—MAGCLA^{TM}.

The values of the parameters and processing variables for the blank simulation appear to have been well chosen, as the trajectories obtained are clearly within what was expected, and there seems to be enough margin to vary the processing variables widely enough to determine their influence.

The values obtained for the exit times of the non-magnetic particles and for the times of collection, in the central collector, of the magnetic particles are low, and their velocity is not too high, which is due to a speed of rotation moderately high and to a high electrical current density (which creates a magnetic force density profile quite high). These results are beneficial when separation–classification of the particles is desired.

Acknowledgement

Fundação para a Ciência e a Tecnologia is acknowledged for its Post-Doc grant SFRH/BPD/6964/2001 (P.A. Augusto).

References

[1] S.-I. Andersson, T. Myrstad, Test of magnetically separated catalysts in an ARCO pilot unit, Appl. Catal. A: Gen. 159 (1–2) (1997) 291–304.
[2] J.M. Rodriguez, A. Macias-Machín, A. Alvaro, J.R. Sanchéz, A.M. Estévez, Removal of iron oxide particles in a gas stream by means of a magnetically stabilized granular filter, Ind. Eng. Chem. Res. 38 (1999) 276–283.
[3] M. Safarikova, I. Safarik, The application of magnetic techniques in biosciences, Magn. Electr. Sep. 10 (4) (2001) 223–252.
[4] P.A. Augusto, T. Castelo-Grande, P. Augusto, Magnetic classification, Miner. Eng. 15 (1–2) (2002) 35–43.
[5] P.A. Augusto, Um novo separador e classificador magnético, Ph.D. Thesis, Departamento de Engenharia Química, Faculdade de Engenharia da Universidade do Porto, 2001.
[6] J.A. Oberteuffer, Magnetic separation: a review of principles, devices, and applications, IEEE Trans. Magn. 10 (2) (1974) 223–238.
[7] P.A. Augusto, Patent 102326-B (PCT filled also).
[8] P.A. Augusto, J.P. Martins, A new magnetic separator and classifier: prototype design, Miner. Eng. 12 (7) (1999) 799–807.
[9] P.A. Augusto, T. Castelo-Grande, P. Augusto, A new magnetic separator and classifier: reducing air pollution and improving the environment, Electron. J. Environ. Agric. Food Chem. 2 (2) (2003).
[10] P.A. Augusto, T. Castelo-Grande, P. Augusto, Magnetic classification in health sciences and in chemical engineering, Chem. Eng. J. 111 (2005) 85–90.
[11] P.A. Augusto, T. Castelo-Grande, P. Augusto, D. Barbosa, A. Estévez, Supporting theory of a new magnetic separator and classifier. Equations and modeling: Part I—Non-magnetic particles, Curr. Appl. Phys., in press.
[12] P.A. Augusto, T. Castelo-Grande, P. Augusto, D. Barbosa, A. Estévez, Supporting theory of a new magnetic separator and classifier. Equations and modeling: Part II—Magnetic particles, Curr. Appl. Phys., in press.
[13] P.A. Augusto, T. Castelo-Grande, P. Augusto, D. Barbosa, A. Estévez, Supporting theory of a new magnetic separator and classifier. Limitting conditions: Part I—Non-magnetic particles, Curr. Appl. Phys., in press.
[14] P.A. Augusto, T. Castelo-Grande, P. Augusto, D. Barbosa, A. Estévez, Supporting theory of a new magnetic separator and classifier. Limitting conditions: Part II—Magnetic particles, Curr. Appl. Phys., in press.
[15] P.A. Augusto, T. Castelo Grande, P. Augusto, Magnetic classification: a new direction for magnetic separation, Ind. Miner. 423 (2002) 52–57.
[16] P.A. Augusto, T. Castelo-Grande, D. Barbosa, A. Estévez, Application of a new magnetic separator and classifier: typical case studies, AIChE J., submitted for publication.